Max-Planck-Institut für Meteorologie

REPORT No. 135

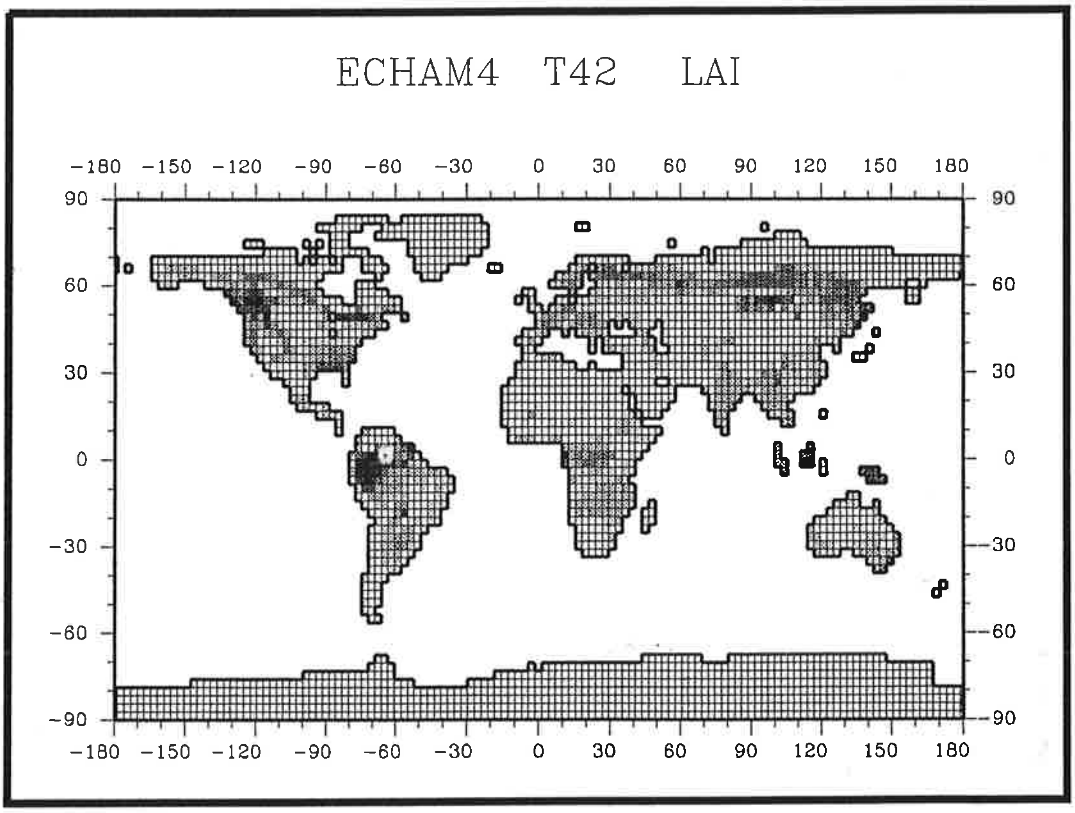

A GLOBAL DATA SET OF LAND-SURFACE PARAMETERS

by

MARTIN CLAUSSEN • ULRIKE LOHMANN
ERICH ROECKNER • UWE SCHULZWEIDA

HAMBURG, June 1994

AUTHORS:

Martin Claussen
Ulrike Lohmann
Erich Roeckner
Uwe Schulzweida

Max-Planck-Institut
für Meteorologie

MAX-PLANCK-INSTITUT
FÜR METEOROLOGIE
BUNDESSTRASSE 55
D-20146 Hamburg
F.R. GERMANY

Tel.: +49-(0)40-4 11 73-0
Telefax: +49-(0)40-4 11 73-298
E-Mail: <name> @ dkrz.d400.de

REPb 135

ISSN 0937-1060

A Global Data Set of Land-Surface Parameters

Martin Claussen
Ulrike Lohmann
Erich Roeckner
Uwe Schulzweida

Max-Planck Institut für Meteorologie
Bundesstr. 55
20146 Hamburg, Fed. Rep. Germany

Abstract

A global data set of land surface parameters is provided for the climate model ECHAM developed at the Max-Planck-Institut für Meteorologie in Hamburg. These parameters are: background (surface) albedo α, surface roughness length z_{0v}, leaf area index LAI, fractional vegetation cover or vegetation ratio c_v, and forest ratio c_F. The global set of surface parameters is constructed by allocating parameters to major ecosystem complexes of Olson *et al.* (1983). The global distribution of ecosystem complexes is given at a resolution of 0.5^0 x 0.5^0. The latter data are compatible with the vegetation types used in the BIOME model of Prentice *et al.* (1992) which is a potential candidate of an interactive submodel within a comprehensive model of the climate system.

1 Introduction

Numerical models of the atmosphere need land-surface parameters which are implicit in the parameterization of energy and momentum fluxes at the atmosphere - ground interface. In the climate model ECHAM, developed at the Max-Planck-Institut für Meteorologie in Hamburg, these parameters are the background albedo α (albedo of snow-free land surfaces), the surface roughness length z_{0v}, the leaf area index LAI, the fractional vegetation cover or vegetation ratio c_v, and the forest ratio c_F which is used to compute the albedo of snow-covered forested areas. (The model physics of ECHAM as well as its validation is described in detail by Roeckner *et al.* (1992).)

In earlier versions of ECHAM (level 1, 2, 3), c_v is inferred from data of Wilson and Henderson-Sellers (1985), and α is derived from satellite data of Geleyn and Preuß (1983). z_{0v} is taken from Baumgartner *et al.* (1977), and c_F is prescribed using data of Matthews (1984). LAI is a global constant $LAI = 4$. As a new version of ECHAM (level 4) is implemented, we decided to provide a new data set of land-surface parameters. The construction of this data set has been guided by the following considerations.

It has been realized that modeling the climate system requires to set up a model system in which the various models of climate subsystems, atmosphere, ocean, and biosphere, are interactively coupled. The interaction between atmosphere and ocean has quite intensively been studied during the last few years (e.g. Cubasch et al. 1992). However, less attention has been paid to the interactive integration of biosphere and atmosphere although the sensitivity of climate simulations to changes in vegetation patterns is well documented (e.g. Mintz, 1984). As a first attempt, Henderson-Sellers (1993) has combined the Holdrige vegetation scheme and the NCAR community climate model. Claussen (1994) has coupled the more advanced BIOME model of Prentice *et al.* (1992) with ECHAM. (The current version of the BIOME model is a static, equilibrium-response model; a global model of vegetation dynamics is not expected to be operational within near future.) Consequently, we decided to construct the new global data set of land-surface parameters by consistenly allocating all parameters to one data set of vegetation. We have chosen the data set of major ecosystem complexes of Olson *et al.* (1983), because this data set is compatible with the vegetation types used in the BIOME model which, as just mentioned, is a potential candidate of an interactive submodel within a comprehensive model of the climate system.

This rather technical note summarizes the new data set of land-surface parameters and reviews the rationale of constructing it.

2 Surface albedo

The background albedo α over snow-free land surfaces is calculated on the basis of three data sets:

- Clear–sky radiances at the top of the atmosphere analysed for one year (Feb. 1985–Jan.1986) of satellite data of the "Earth Radiation Budget Experiment" (ERBE; Ramanathan *et al.,* 1989). The spatial resolution is 2.5° × 2.5°.
- Surface albedo for vegetated areas allocated to a high–resolution 0.5° × 0.5° global distribution of major ecosystem complexes of Olson *et al.* (1983) - see Section 2.2.
- Surface albedo as deduced by Dormann and Sellers (1989) from a radiative transfer model on the basis of vegetation data such as leaf area index and leaf optical properties.

2.1 Satellite-derived surface albedo

In order to derive the surface albedo from the ERBE clear–sky fluxes at the top of the atmosphere an atmospheric correction has to be applied. The procedure involves a climate simulation over the respective period (using observed sea surface temperatures specified for each month) performed with the ECHAM3/T42 model (Roeckner *et al.,* 1992). In this approach we assume that the differences between the simulated and the observed clear–sky albedo at the top of the atmosphere (TOA) are caused merely by the inadequate surface albedo specified in the model simulation (Geleyn and Preuß, 1983). This assumption seems to be justified, because the surface albedo is by far the most important contributor to the planetary clear–sky albedo. A practical problem, however, is the identification of clear–sky scenes from the ERBE measurements which is difficult (sometimes impossible) in areas with persistent cloudiness.

The procedure involves the following steps where all fluxes represent annual averages.

2.1.1 Solar constant adjustment

Since the solar constants used in ERBE and ECHAM are not identical, the reflected solar radiation measured by ERBE has been adjusted according to the solar irradiance $S^{\downarrow}(M)$ used in the ECHAM model.

$$S^{\uparrow}(E)^{\star} = \alpha_0(E) \cdot S^{\downarrow}(M) \tag{1}$$

where (E) refers to ERBE and (M) to the ECHAM model. $S^{\uparrow}(E)^{\star}$ is the corrected upward directed solar flux which would be identical to the measured flux $S^{\uparrow}(E)$ if the irradiances would be the same ($S^{\downarrow}(M) = S^{\downarrow}(E)$), and α_0 is the planetary clear-sky albedo. The model error at TOA,

$$\delta S^{\uparrow} = S^{\uparrow}(M) - S^{\uparrow}(E)^{\star} \quad , \tag{2}$$

is used to correct the simulated flux reflected at the surface,

$$S_s^{\uparrow}(M)^{\star} = S_s^{\uparrow}(M) - \delta S^{\uparrow} \tag{3}$$

where the subscript "s" denotes the respective flux at the surface, so that the ERBE–derived surface albedo is given as

$$\alpha_E = \frac{S_s^{\uparrow}(M)^{\star}}{S_s^{\downarrow}(M)} = \frac{S^{\uparrow}(E)^{\star} - S_a^{\uparrow}(M)}{S_s^{\downarrow}(M)} \tag{4}$$

where $S_a^{\uparrow}(M) = S^{\uparrow}(M) - S_s^{\uparrow}(M)$ is the atmospheric correction.

2.1.2 Cloud correction

Although the method outlined above is based on clear–sky fluxes, a correct identification of the clear–sky scenes is not always possible (Ramanathan *et al.,* 1989). The above analysis leads to poor results over the tropical rainforests ($\alpha_E > 0.20$), which are characterized by large cloud cover, primarily during the day. In these areas we therefore replace the estimate Eq.4 by a value of 0.12 which is typical for tropical rainforests throughout the year (Dormann and Sellers, 1989, Gash and Shuttleworth, 1991).

2.1.3 Snow correction

If the ERBE data or the model simulation suggest a snow cover during a particular month at a particular grid point, the respective surface flux is rejected, and the time averaging is done only over the snow–free period. In areas with persistent snow cover throughout the year, a surface albedo of 0.17 is specified which is close to the annual mean value for tundra (Dormann and Sellers, 1989).

2.2 Albedo of vegetated surfaces

For estimating the albedo α_v of purely vegetated surfaces, we basically follow the approach outlined by Henderson-Sellers *et al.* (1986). Henderson-Sellers *et al.* (1986) redefine the major ecosytem complexes i of Olson *et al.* (1983) as proportions f_{ij} of 13 simple surface types j - see Table 2. (in Table 2, f_{ij} is given in per cent.) For the reader's convenience, the original notation of ecosytem complexes in Olson *et al.* (1983) and the abreviated notation used in this report are given in Table 1. In Table 3, the simple surface types are defined.

In Henderson-Sellers *et al.* (1986), the surface albedo α_i, including albedo of bare soil and vegetation, is given by

$$\alpha_i = \sum_j f_{ij}\alpha_{sj} \qquad , \tag{5}$$

where α_{sj} is the average annual albedo of the simple surface type j. We deviate from this original approach in several aspects.

We compute α_{vi}, the albedo just due to vegetation, by

$$\alpha_{vi} = \frac{\sum_j f_{ij}\alpha_{sj}}{1 - f_{ib}} \qquad , \tag{6}$$

where

$$f_{ib} = f_{i1} + f_{i13}$$

is the proportion of desert and bare soil assigned to the ecosystem complex i. Eq.6 is not applied to Sand Desert and Polar Desert for which $f_{ib} = 1$. In these cases, we specify α_{vi} of semi desert and tundra, respectively, as dummy values. For Lakes, we also provide a dummy value of $\alpha_{vi} = 0.07$ as the albedo of water surface is computed as function of solar zenith angle in ECHAM.

The albedo α_{sj} of simple surface types is listed in Table 3. Only for simple surface types 3, 4, 7, 9, 11, we use the original specification of Henderson-Sellers *et al.* (1986). For 10, cultivation, we use a value which is closer to the average of albedo values for several explicitly defined types of cultivation given in Wilson and Henderson-Sellers (1985). Likewise, for 12, semidesert, we use a value which is closer to Wilson and Henderson-Sellers (1985) specification. For 2, 5, 6, tundra, grassland with tree cover, deciduous forest, we use more recent estimates of Dorman and Sellers (1989). For 8, rain forest, we refer to recent measurements of Gash and Shuttleworth (1991). No values are assigned to 1 and 13, desert and bare soil, because the information of bare soil should be incorporated by using the ERBE data - see next Section 2.3. (Here, we consider desert as vegetationless desert in contrast to semidesert.)

The resulting values of α_{vi} are listed in Table 7. In the following, the index i will be droped.

2.3 Blended surface albedo

Finally, the surface albedo α is a blend of α_v and α_E,

$$\alpha = c_v \cdot \alpha_v + (1 - c_v) \cdot \alpha_E \quad (7)$$

where c_v is the fractional vegetation cover or vegetation ratio. Specification of c_v will be discussed in Section 5.

The distribution of surface albedo according to Eq.7 is shown in Figure 1, and in Figure 2, the albedo originally used in ECHAM.

Considering the many uncertainties involved in the procedure outlined, we have not attempted to calculate a seasonal cycle of the surface albedo. The annual mean albedo according to Eq.7 is available at five resolutions (T21, T42, T63, T106, i.e. $5.625° \times 5.625°$, $2.8125° \times 2.8125°$, $1.875° \times 1.875°$, and $1.125° \times 1.125°$, respectively, and $0.5° \times 0.5°$). We have to mention, however, that the contribution from the satellite data is interpolated in each case from the relatively coarse ERBE grid of $2.5° \times 2.5°$ which is similar to T42 resolution. Consequently, the satellite information is about the same for T42, T63 and T106 resolution.

3 Vegetation roughness

Momentum and energy fluxes at the atmosphere - ground interface in ECHAM are controled by a roughness length z_0. z_0 consists of three parts: a roughness length z_{oro} computed from the variance of orography, a roughness length z_{urb} of urban areas with tall buildings, and z_{0v}, a roughness length of vegetation and land use apart from urban areas. According to Tibaldi and Geleyn (1981), $z_0 = \sqrt{z_{oro}^2 + z_{urb}^2 + z_{0v}^2}$. Originally, z_{0v} was taken from Baumgartner *et al.* (1977) who provided estimates at a resolution of $5° \times 5°$. Here, we attempt to establish a new global data set of z_{0v} at a much finer resolution.

For estimation of z_{0v}, we follow the approach of Henderson-Sellers *et al.* (1986). As outlined in Section 2.2, the major ecosystem complexes of Olson *et al.* (1983) are redefined as 13 simple surface types (see Table 2). Subsequently, we assign values z_{0sj} to each simple surface type j. However, in contrast to Henderson-Sellers *et al.* (1986), we include more recent results by Wieringa (1991, 1992). Wieringa (1991, 1992) provides a comprehensive review of several hundred papers on measurements of roughness length, and he carefully selects only the best measurements which fullfill certain qualitiy standards. We allocate Wieringa's (1991) update of the original Davenport classification of roughness to Henderson-Sellers' *et al.* (1986) simple surface types (see Table 4). Subsequently, we average roughness lengths following the so-called concept of blending height (e.g. Wieringa, 1986, Mason, 1988, Claussen, 1991). Not z_{0sj} values, but drag coefficients $c_{dj} = (\kappa / ln(z_b/z_{0sj}))^2$ are averaged, where c_d are taken at the so-called blending height z_b. This leads to

$$\frac{1}{ln^2\left(\frac{z_b}{z_{0vi}}\right)} = \sum_j \left(\frac{f_{ij}}{ln^2\left(\frac{z_b}{z_{0sj}}\right)} \right) \quad . \tag{8}$$

Here, we choose $z_b \simeq 100$m as an order-of-magnitude guess (e.g. Claussen, 1990, Wieringa, 1992). Exceptions from this rule are estimates for Antarctica, Sand Desert and Polar Desert, where we directly, without averaging over simple surface types, prescribe $z_{0vi} = 0.001$m which is a value in between Wieringa's (1992) suggestions for "flat desert" and "flat snow field" on the smooth side and "rough ice field" and "fallow ground" on the rough side. Results are shown in Table 7. In the following, the index i in z_{0vi} is droped.

The new z_{0v} are listed in Table 7. These values are compared with the original ones by Baumgartner *et al.* (1977) in Figures 3 and 4, respectively. It turns out that both global distributions of z_{0v} agree by and large. There are rough regions as the rain forests in the Amazon Basin, in the Congo Basin, and in Indonesia. Also, a rough belt is seen in the Northern Hemisphere due to boreal forests. Generally, Baumgartner's *et al.* values seem to be a little bit larger than the new z_{0v}. In fact, that could have been anticipated, because Baumgartner's *et al.* regression formula by which z_{0v} is related to the height of vegetation becomes unrealistically large at $z_{0v} > 0.1$m (Wieringa, 1992).

First sensitivity tests reveal that use of the new z_{0v} instead of Baumgartner's *et al.* values marginally affects climate simulations at coarse resolution (T42). That is no surprise because both distributions of roughness length are similar, and, by comparison with z_{oro} and z_{urb}, z_{0v} is the smallest contribution to the overall z_0. The new and old global patterns of z_0 are given in Figure 5 and 6, respectively.

4 Forest ratio

In the earlier versions of ECHAM, a forest ratio c_F is specified from the vegetation data of Matthews (1984). These data indicate whether there is a forest or not. Here, we attempt to improve on this information by using Olson's *et al.* (1983) description of forests. Olson *et al.* (1983) distinguish four major categories of ecosystem complexes: forest and woodland, interrupted woods, nonwoods, and wetland. The first landscape complex is considered to be covered by more than 60% forest area, while "nonwoods" include less than 20% forest area.

Moreover, we specify a forest ratio c_F which is consistent with the vegetation ratio c_v (see next Section 5). We require that $c_F \leq c_v$. This relation should be valid for evergreen plants throughout the year, and for deciduous plants, during summer. In winter, c_v could become smaller than c_F for the following reason. c_F just indicates the fractional cover of trees regardless whether they are physiologically active not. c_F is used to modify the albedo of snow covered forests. In contrast, c_v indicates the fractional cover of live plants which are able to modify evaporation by their stomata.

For ecosystem complexes which are in the category "forest and woodland", we have chosen $0.6 \leq c_F \leq 1.0$. In particular, Broadleaved Evergreen, Warm Conifer, Rain Forest are assumed to be closed forest with $c_F = 0.95$. For Cool Conifer and Warm Deciduous, which are closed forest, $c_F = 0.9$ and $c_F = 0.85$, respectively, to obey the rule $c_F \leq c_v$. Tropical Seasonal is described as to favor burning and farm patches, hence we specify $c_F = 0.9$ assuming that farm patches are small. Otherwise, the areas in question would have been assigned to man-used forest/field complexes. Cool Mixed and Warm Mixed are described as closed to open hardwood, therefore, $c_F = 0.8$. Main and Southern Taiga are considered to be disturbed in large areas by fires, pests, and harvest, hence, $c_F = 0.8$. For Tropical Dry, $c_F = 0.6$ is assumed, because it is described as transitional to savannas, which is referred to as interrupted woods for which $c_F < 0.6$.

For Tropical Montane, we assume $c_F = 0.5$, and for Savanna, Northern Taiga, Low Shrub, Succulent, and Mediterranean Types, $c_F = 0.4$. The latter differentation should reflect Olson's *et al.* (1983) description of Savanna as "trees and shrubs scattered in grassy undercover", Northern Taiga as "stunted and open boreal conifer", and the latter three as "woods / scrub / grass complexes"

For forest/field complexes, Olson *et al.* (1983) assume 60%-40% of nonwoods vegetation, for field/woods, 80%-60%, and for "Nonwoods", 100%-80%. Accordingly, we specified for Cool and Warm Field/Woods $c_F = 0.3$, and Cool and Warm Woods/Fields, $c_F = 0.5$. In the ("nonwood") category of grass and shrub complexes, Wooded Tundra is described to favor existence of some dwarfed trees, hence we assume $c_f = 0.2$ for this tundra type. In the category of major wetlands, we assume that for Mangroves $c_F = 0.9$, because this generally dense forest is described as being modified by natural shore widening or erosion in some places.

The new values of c_F are listed in Table 7. Their global distribution is plotted in Figure 7. The old c_F distribution is given in Figure 8. It is seen that both maps (Figure 7 and 8) reveal a similar structure. They show dense forests in the Amazon Basin, in the Congo Basin, in Indonesia, in Siberia, and in North America/Canada. Striking differences are detectable for Europe, China and India which are considered densely forested in the old data set and only moderately, in the new data set. This is rather surprising because the cultivation intensity as given by Matthews (1984) - from which the former values of c_F are deduced - is large in these areas.

5 Vegetation ratio and leaf area index

Allocation of vegetation ratio c_v and leaf area index LAI to vegetation types or ecosystem complexes is just an ad-hoc attempt because both are rather poorly correlated (Esser, Univ. Gießen, personal communication). It seems more reasonable to infer LAI and c_v from data of net primary production (npp) of vegetation. The latter could be inferred from observations or results of terrestrial biogeochemical models (TBM). Since this has not yet been tested, the provisional data of c_v and LAI will be used.

c_v and LAI values are constructed in the following manner. We use values assigned to vegetation types by Lieth and Esser (cited in Heise *et al.,* 1988) by allocating Olson's *et al.* (1983) ecosytem complexes to Lieth and Esser's vegetation types (see Table 5 and 6, respectively). There are two values for both c_v and LAI, one for the growing season and one for the season of dormancy, labeled g and d, respectively. In ECHAM, an annual average of c_v and LAI has to be specified which we take as arithmetic average of the corresponding g and d values.

Some of the ecosystem complexes do not appear as vegetation type in Table 5. These are agricultural ecosystems, such as cool and warm crops etc., and coastal edges. For these, we provide a first guess which is broadly consistent with Lieth and Esser's suggestions.

The new values of c_v and LAI are given in Table 8; furthermore, the new and the old global distribtuion of c_v is shown in Figure 9 and 10, respectively. The new global distribution of LAI is presented in Figure 13.

By comparing Figures 9 and 10, it appears that the new values of c_V are generally smaller than the old ones. We believe that the old data set exaggerates c_v. It seems hardly possible that, in most parts of the world, c_v is larger than 0.8 during all seasons. Moreover, the occurrence of vegetation at the north shore of Greenland is surprising because small plant, grass and lichen, are expected just at the eastern and western coasts. The values of c_v are closer to the new c_v during the growing season. This is seen when comparing Figure 10 with the global distribution of maximum values of c_v depicted in Figure 11. For the purpose of illustration, the minimum values of c_v are plotted in Figure 12.

6 Aggregation problems

The new data set of land-surface parameters α_v, z_{0v}, c_F, c_v, LAI is available at a resolution of 0.5°× 0.5°. Also the blended surface albedo α can be given at that resolution; however, as mentioned in Section 2.3, α_E which is implicit in α, is just interpolated from a 2.5°× 2.5° data set.

To get a data set of land-surface parameters at coarser resolution, parameters have to be aggregated. Here, it is recommended to simply average parameters α_v, c_F, c_v, LAI. For z_{0v}, the concept of blending height, i.e. an aggregation formula as in Equation 8, should be used. A reasoning for this procedure is given in Claussen (1993).

7 Concluding remarks

The new global data set of land-surface parameters for use in the climate model ECHAM level 4 has been set up by consistenly allocating all parameters to the major ecosystem complexes of Olson *et al.* (1983). The latter data are compatible with the vegetation types used in the BIOME model of Prentice *et al.* (1992) which is a potential candidate of an interactive submodel within a comprehensive model of the climate system.

As Henderson-Sellers *et al.* (1986) state in their conclusions "It is nonproductive to attempt to answer questions such as Which is the best global land-surface data archive currently available?" All of them are arbitrary to some extent and have been derived from similar, or identical, sources. However, not all data sets are consistent in this sense that a change in vegetation implies a consistent change in all surface parameters. Here, we have constructed such a data set of land-surface parameters - a data set which is consistent with Olson's *et al.* definition of ecosystem complexes.

The global distribution of new land-surface parameters has already been used in a few test simulations with ECHAM. It seems to "work" properly. Nevertheless, a few modifications are desirable. LAI, c_v, and presumably also c_F are provisional data. Instead of allocating these parameters to ecosystems or biomes, it is suggested to compute them from TBMs, preferably from TBMs into which the BIOME model of Prentice *et al.* (1992) is incorporated. This approach would also allow for computing a realistic seasonal cycle of LAI and c_v, and, subsequently, α. However, this has not yet been achieved and remains a challenging task for further improvement.

References

Baumgartner A, Mayer H and Metz W (1977) Weltweite Verteilung des Rauhigkeitsparameters z_0 mit Anwendung auf die Energiedissipation an der Erdoberfläche. Meteorolog.Rdsch. 30: 43-48.

Claussen M (1990) Area-averaging of surface fluxes in a a neutrally stratified, horizontally inhomogeneous atmospheric boundary layer. Atmos. Environ. 24a: 1349-1360.

Claussen M (1991) Estimation of areally-averaged surface fluxes. Boundary-Layer Meteorol. 54: 387-410

Claussen M (1993) Flux aggregation at large scales: On the limits of validity of the concept of blending height. J. Hydrology, accepted.

Claussen M (1994) On coupling global biome models with climate models. Clim. Res., submitted, available as Report 131, Max-Planck-Institut für Meteorologie, Hamburg, F.R.G.

Claussen M and Esch M (1994) Biomes computed from simulated climatologies. Climate Dyn. 9: 235-243.

Cubasch U, Hasselmann K, Höck H, Maier-Reimer E, Mikolajewicz U, Santer BD, Sausen, R (1992) Time-dependent greenhouse warming computations with a coupled ocean-atmosphere model. Climate Dyn. 8: 55-69.

Dorman JL, Sellers PJ (1989) A global climatology of albedo, roughness length adn stomatal resistance for atmospheric general circulation models as represented by the Simple Biosphere Model (SiB). J. Appl. Meteorol. 28: 833-855.

Gash JHC, Shuttleworth WJ (1991) Tropical deforestation: albedo and the surface-energy balance. Climatic Change 19: 123-133.

Geleyn J-F and Preuß HJ (1983) A new dataset of sattelite-derived surface albedo values for operational use at ECMWF. Arch.Meteor.Geophys.Bioclim., Ser.A 32: 353-359.

Henderson-Sellers A (1993) Continental vegetation as a dynamic component of global climate model: a preliminary assessment. Climatic Change 23: 337-378

Heise E, Jacobs W, Ketterer M, Renner V (1988) Klimasimulation mit atmosphärischen Modellen im Zeitskalenbereich von Monaten. Abschlußbericht des BMFT-Projektes KF 2012 8, Deutscher Wetterdienst, Offenbach.

Henderson-Sellers A (1993) Continental vegetation as a dynamic component of global climate model: a preliminary assessment. Climatic Change 23: 337-378.

Henderson-Sellers A, Wilson MF, Thomas G, Dickinson RE (1986) Current global land-surface data sets for use in climate-related studies. NCAR Technical Note NCAR/TN-272+STR, National Center for Atmospheric Research, Boulder, Colorado.

Leemans R and Cramer W (1991) The IIASA database for mean monthly values of temperature, precipitation, and cloudiness on a global terrestrial grid. IIASA Research Report RR-91-18, Laxenburg, Austria.

Martin P (1993) Vegetation responses and feedbacks to climate: a review of models and processes. Climate Dyn. 8: 201-210.

Mason PJ (1988) The formation of areally-averaged roughness lengths. Q. J. R. Meteorol. Soc. 114: 399-420.

Matthews E (1984) Vegetation, land-use and seasonal albedo data sets: documentation of archived data tape. NASA Technical Memorandum 86107, Goddard Space Flight Center, New York.

Mintz Y (1984) The sensitivity of numerically simulated climates to land-surface boundary conditions. in: Houghton J The global climate. Cambridge Univ. Press.

Olson JS, Watts JA, Allison LJ (1983) Carbon in live vegetation of major world ecosystems. ORNL-5862, Oak Ridge National Laboratory, Oak Ridge.

Prentice IC, Cramer W, Harrison SP, Leemans R, Monserud RA, and Solomon AM (1992) A global biome model based on plant physiology and dominance, soil properties and climate. Journal of Biogeography 19: 117-134.

Ramanathan V, Cess RD, Harrison EF, Minis P, Barkstrom BR Ahmad E, Hartmann D (1989) Cloud-radiative forcing and climate: results from the Earth Radiation Budget Experiment. Science 243: 57-63.

Roeckner E, Arpe K, Bengtsson L, Brinkop S, Dümenil L, Kirk E, Lunkeit F, Esch M, Ponater M, Rockel B, Sausen R, Schlese U, Schubert S, Windelband M (1992) Simulation of the present-day climate with the ECHAM model: Impact of model physics and resolution. Report 93, Max-Planck-Institut für Meteorologie, Hamburg.

Tibaldi S and Geleyn J-F (1981) The production of a new orography, land-sea mask and associated climatological surface fields for operational purposes. ECMWF Tech.Memo. 40.

Wieringa J (1986) Roughness-dependent geographical interpolation of surface wind speed averages. Quart. J. R. Met. Soc. 112: 867-889.

Wieringa J (1991) Updating the Davenport roughness classification. J. Wind Engin. Industr. Aerodyn. 41-44: 357-368.

Wieringa J (1992) Representative roughness parameters for homogeneous terrain. Boundary-Layer Meteorol. 63: 323-363.

Wilson MF and Henderson-Sellers A (1985) A global archive of land cover and soils data for use in general circulation climate models. Journal of Climatology 5: 119-143.

Table 1: Allocation of Land Types to Olson and Watts' Ecosystem Complexes

Land Type	Major Ecosystem Complex
Antarctica	Antarctic Desert
Sibirian Parks	Siberian Parklands, Tibetian Meadows
Main Taiga	Main Taiga
Cool Conifer	Cool Conifer
Cool Mixed	Cool Hardwood-Conifer
Warm Mixed	Deciduous Warm Woods with Conifer, Partly Evergr. Broad-Leaved and Subtrop. Conifer, Evergreen Broad-Leaved and Conifer
Warm Deciduous	Deciduous Forest
Broadleaved Evergreen	Broad-Leaved Evergr. or Partly Deciduous Forest, Broad-Leaved South-Temperate Forest
Warm Conifer	Warm or Hot Conifer
Tropical Montane	Tropical Montane Complexes
Tropical Seasonal	Tropical Seasonal Forest
Cool Crops	Cool or Cold Farms, Towns
Warm Farms	Warm or Hot Farms, Towns
Tropical Dry	Tropical Dry Forest and Woodland
Rain Forest	Evergreen Equatorial Forest
Paddyland	Paddyland
Warm Irrigated Dry	Warm, Hot Irrigated Dryland Row Crops
Cold Irrigated Dry	Cold Irrigated Dryland Row Crops
Cool Irrigated Dry	Cool Irrigated Dryland Row Crops
Cool Grass	Cool Grassland/Shrub
Warm Grass	Warm or Hot Shrub and Grassland
Savanna	Tropical Savanna and Woodland
Bogs	Bog/Mire of Cool or Cold Climates
Mangroves	Mangrove/Tropical Swamp Woods
Low Shrub	Other Dry or Highland Tree or Shrub Types
Mediterranean Types	Mediterranean Types
Semiarid Woods	Semiarid Woodland and Low Forest
Succulent	Succulent and Thorns Woods and Shrubs
Sand Desert	Sand Desert
Hot Desert	Desert and Semidesert
Cool Desert	Semidesert Shrub
Tundra	Tundra
Polar Desert	Polar or Rock Desert
Cool Field/Woods	Second-Growth Woods and Field Mosaics ...... : Field/Woods (temperate)
Warm Woods/Field	- " - : Forest/Field (tropical/subtropical)
Cool Woods/Field	- " - : - " - (temperate/boreal)
Warm Field/Woods	- " - : Field/Woods (tropical)
Southern Taiga	Southern Continental Taiga
Northern Taiga	Northern or Maritime Taiga
Wooded Tundra	Wooded Tundra and Timberline
Heath	Heath and Moorland
Swamp/Marsh	Swamp/Marsh
Coastal Edges	Shore and Hinterland Complexes
Ice	Ice
Lakes	Major Lakes

Table 2: Redefinition of Land Types i as proportions f_{ij} of Simple Surface Types j

Land Type	Simple Surface Type												
	1	2	3	4	5	6	7	8	9	10	11	12	13
Antarctica	0	0	0	0	0	0	0	0	100	0	0	0	0
Sibirian Parks	0	0	75	25	0	0	0	0	0	0	0	0	0
Main Taiga	0	0	0	0	0	0	100	0	0	0	0	0	0
Cool Conifer	0	0	0	0	0	0	100	0	0	0	0	0	0
Cool Mixed	0	0	0	0	0	50	50	0	0	0	0	0	0
Warm Mixed	0	0	10	0	0	60	20	0	0	0	0	0	10
Warm Deciduous	0	0	0	0	0	100	0	0	0	0	0	0	0
Broadleaved Evergreen	0	0	10	0	0	40	40	0	0	0	0	0	10
Warm Conifer	0	0	0	0	0	0	100	0	0	0	0	0	0
Tropical Montane	0	0	0	10	20	30	30	0	0	0	0	0	10
Tropical Seasonal	0	0	0	0	0	0	0	100	0	0	0	0	0
Cool Crops	0	0	0	0	0	0	0	0	0	100	0	0	0
Warm Farms	0	0	0	0	0	0	0	0	0	100	0	0	0
Tropical Dry	0	0	20	0	0	0	70	0	0	0	0	0	10
Rain Forest	0	0	0	0	0	0	0	100	0	0	0	0	0
Paddyland	0	0	0	0	0	0	0	0	0	50	50	0	0
Warm Irrigated Dry	30	0	0	0	0	0	0	70	0	0	0	0	0
Cold Irrigated Dry	0	0	0	0	0	0	0	0	0	70	0	0	30
Cool Irrigated Dry	0	0	0	0	0	0	0	0	0	70	0	0	30
Cool Grass	0	0	50	50	0	0	0	0	0	0	0	0	0
Warm Grass	0	0	0	100	0	0	0	0	0	0	0	0	0
Savanna	10	0	0	0	80	10	0	0	0	0	0	0	0
Bogs	0	0	0	0	0	0	0	0	0	0	100	0	0
Mangroves	0	0	0	0	0	0	0	75	0	0	25	0	0
Low Shrub	0	0	0	30	0	0	40	0	0	0	0	0	30
Mediterranean Types	0	0	0	20	0	0	60	0	0	0	0	0	20
Semiarid Woods	60	0	0	20	20	0	0	0	0	0	0	0	0
Succulent	30	0	0	50	0	0	0	0	0	0	0	0	20
Sand Desert	100	0	0	0	0	0	0	0	0	0	0	0	0
Hot Desert	100	0	0	0	0	0	0	0	0	0	0	0	0
Cool Desert	0	0	0	0	0	0	0	0	0	0	0	100	0
Tundra	0	100	0	0	0	0	0	0	0	0	0	0	0
Polar Desert	100	0	0	0	0	0	0	0	0	0	0	0	0
Cool Field/Woods	0	0	0	50	0	0	0	0	0	50	0	0	0
Warm Woods/Field	0	0	0	50	50	0	0	0	0	0	0	0	0
Cool Woods/Field	0	0	0	50	50	0	0	0	0	0	0	0	0
Warm Field/Woods	0	0	0	50	0	0	0	0	0	50	0	0	0
Southern Taiga	0	0	0	0	40	60	0	0	0	0	0	0	0
Northern Taiga	0	0	25	0	0	0	50	0	0	0	0	0	25
Wooded Tundra	0	60	0	40	0	0	0	0	0	0	0	0	0
Heath	0	0	0	100	0	0	0	0	0	0	0	0	0
Marsh/Swamp	0	0	0	0	0	0	0	0	0	0	100	0	0
Coastal Edges	0	0	0	50	0	0	0	0	0	0	0	0	50
Ice	0	0	0	0	0	0	0	0	100	0	0	0	0
Lakes	0	0	0	0	0	0	0	0	0	0	0	0	0

Table 3: Allocation of vegetation albedo to simple surface types

j	simple surface type	α_{sj}
1	desert	-
2	tundra	0.17
3	grassland	0.19
4	grassland with shrub cover	0.20
5	grassland with tree cover	0.16
6	deciduous forest	0.16
7	evergreen forest	0.13
8	rain forest	0.12
9	ice	0.70
10	cultivation	0.18
11	bog or marsh	0.12
12	semidesert	0.28
13	bare soil	-

Table 4: Allocation of roughness lengths to simple surface types

j	simple surface type	Davenport class.	z_{0vj} (m)
1	desert	smooth	0.005
2	tundra	open	0.03
3	grassland	open	0.03
4	grassland with shrub cover	roughly open	0.1
5	grassland with tree cover	rough	0.25
6	deciduous forest	closed	1.00
7	evergreen forest	closed	1.00
8	rain forest	chaotic	2.00
9	ice	smooth	0.005
10	cultivation	roughly open	0.1
11	bog or marsh	open	0.03
12	semidesert	smooth	0.005
13	bare soil	smooth	0.005

Table 5: Allocation of Land Types to Lieth and Esser's Vegetation Types

Land Type	Vegetation Type
Antarctica	-
Sibirian Parks	Boreal shrub formation
Main Taiga	Boreal evergreen coniferous forest
Cool Conifer	Temperate evergreen coniferous forest
Cool Mixed	Temperate woodland
Warm Mixed	Subtropical deciduous forest
Warm Deciduous	temperate deciduous forest
Broadleaved Evergreen	Subtropical evergreen forest
Warm Conifer	Subtropical evergreen forest
Tropical Montane	Tropical paramo woodland
Tropical Seasonal	Tropical dry lowland forest
Cool Crops	-
Warm Farms	-
Tropical Dry	Tropical dry lowland forest
Rain Forest	Tropical moist lowland forest
Paddyland	-
Warm Irrigated Dry	-
Cold Irrigated Dry	-
Cool Irrigated Dry	-
Cool Grass	Temperate steppe and meadow
Warm Grass	Subtropical steppe and grassland
Savanna	Tropical savanna
Bogs	Temperate bog and tundra
Mangroves	Mangroves
Low Shrub	Temperate shrub formation
Mediterranean Types	Mediterran shrub and woodland
Semiarid Woods	Subtropical savanna
Succulent	Xeromorphic formation
Sand Desert	-
Hot Desert	Subtropical semidesert
Cool Desert	Subtropical semidesert
Tundra	Herbaceous tundra
Polar Desert	-
Cool Field/Woods	-
Warm Woods/Field	-
Cool Woods/Field	-
Warm Field/Woods	-
Southern Taiga	Boreal deciduous forest
Northern Taiga	Boreal woodland
Wooded Tundra	Woody tundra
Heath	Boreal shrub formation
Swamp/Marsh	Azonal formation
Coastal Edges	-
Ice	-
Lakes	-

Table 6: Allocation of Vegetation ratio, Leaf Area Index to Lieth and Esser's vegetation types

Vegetation Type	c_v		LAI	
	g	d	g	d
Subtropical semidesert	0.15	0.0	0.5	0.0
Subtropical savanna	0.34	0.0	1.2	0.0
Temperate steppe and meadow	0.44	0.0	1.5	0.0
Subtropical steppe and grassland	0.44	0.0	1.5	0.1
Tropical savanna	0.53	0.30	1.9	1.0
Herbaceous tundra	0.55	0.0	2.1	0.0
Temperate bog and tundra	0.60	0.0	2.5	0.1
Woody tundra	0.70	0.15	3.2	0.5
Boreal shrub formation	0.73	0.0	3.5	0.1
Boreal woodland	0.73	0.0	3.5	0.1
Azonal formation	0.73	0.67	3.5	3.0
Temperate woodland	0.76	0.0	3.8	0.1
Mediterran shrub and woodland	0.80	0.67	4.3	3.0
Temperate shrub formation	0.85	0.0	4.7	0.1
Boreal deciduous forest	0.86	0.0	4.8	0.1
Xeromorphic formation	0.86	0.30	4.8	1.0
Tropical paramo woodland	0.86	0.77	4.8	4.0
Temperate deciduous forest	0.88	0.0	5.2	0.1
Boreal evergreen coniferous forest	0.91	0.91	6.0	6.0
Subtropical deciduous forest	0.93	0.30	7.0	1.0
Mangroves	0.95	0.95	9.0	9.0
Temperate evergreen coniferous forest	0.96	0.95	9.2	9.0
Tropical moist lowland forest	0.96	0.96	9.3	9.3
Subtropical evergreen forest	0.99	0.97	9.9	9.5

Table 7: Area, Roughness Length, Forest Ratio, and Average Annual Albedo

Land Type	Area	$z_{0v}(m)$	c_F	α_v
Antarctica	13.0	0.001	0.	0.70
Sibirian Parks	.9	0.04	0.	0.19
Main Taiga	4.8	1.0	0.8	0.13
Cool Conifer	2.8	1.0	0.9	0.13
Cool Mixed	1.8	1.0	0.8	0.15
Warm Mixed	1.7	0.68	0.8	0.16
Warm Deciduous	1.0	1.0	0.85	0.16
Broadleaved Evergreen	.5	0.68	0.95	0.15
Warm Conifer	.7	1.0	0.95	0.13
Tropical Montane	.6	0.55	0.5	0.15
Tropical Seasonal	5.2	2.0	0.9	0.12
Cool Crops	3.0	0.1	0.	0.18
Warm Farms	9.3	0.1	0.	0.18
Tropical Dry	4.7	0.55	0.6	0.14
Rain Forest	5.2	2.0	0.95	0.12
Paddyland	2.0	0.06	0.	0.15
Warm Irrigated Dry	.5	0.05	0.	0.18
Cold Irrigated Dry	.5	0.05	0.	0.18
Cool Irrigated Dry	.5	0.05	0.	0.18
Cool Grass	3.9	0.06	0.	0.19
Warm Grass	17.3	0.1	0.	0.20
Savanna	6.7	0.25	0.4	0.16
Bogs	.9	0.03	0.	0.12
Mangroves	1.0	1.29	0.9	0.12
Low Shrub	2.6	0.26	0.4	0.16
Mediterranean Types	1.0	0.46	0.4	0.15
Semiarid Woods	.9	0.04	0.3	0.18
Succulent	4.0	0.03	0.4	0.20
Sand Desert	5.2	0.001	0.	0.28
Hot Desert	11.0	0.005	0.	0.28
Cool Desert	2.0	0.005	0.	0.28
Tundra	11.0	0.03	0.	0.17
Polar Desert	.2	0.001	0.	0.17
Cool Field/Woods	.7	0.1	0.3	0.19
Warm Woods/Field	1.7	0.17	0.5	0.18
Cool Woods/Field	3.5	0.17	0.5	0.18
Warm Field/Woods	1.3	0.1	0.3	0.19
Southern Taiga	2.4	0.65	0.8	0.16
Northern Taiga	4.4	0.31	0.4	0.15
Wooded Tundra	1.7	0.05	0.2	0.18
Heath	.2	0.1	0.	0.20
Marsh/Swamp	.6	0.03	0.	0.12
Coastal Edges	.4	0.03	0.	0.20
Ice	2.0	0.005	0.	0.70
Lakes	3.2	0.0002	0.	0.07

Table 8: Vegetation Ratio, Leaf Area Index

Land Type	c_v		LAI	
	g	d	g	d
Antarctica	0.0	0.0	0.	0.
Sibirian Parks	0.73	0.0	3.5	0.1
Main Taiga	0.91	0.91	6.0	6.0
Cool Conifer	0.96	0.95	9.2	9.0
Cool Mixed	0.76	0.0	3.8	0.1
Warm Mixed	0.93	0.30	7.0	1.0
Warm Deciduous	0.88	0.0	5.2	0.1
Broadleaved Evergreen	0.99	0.97	9.9	9.5
Warm Conifer	0.99	0.97	9.9	9.5
Tropical Montane	0.86	0.77	4.8	4.0
Tropical Seasonal	0.91	0.60	6.0	2.5
Cool Crops	0.90	0.0	2.5	0.
Warm Farms	0.90	0.10	4.5	1.0
Tropical Dry	0.91	0.60	6.0	2.5
Rain Forest	0.96	0.96	9.3	9.3
Paddyland	0.90	0.10	4.5	0.
Warm Irrigated Dry	0.60	0.0	4.0	0.
Cold Irrigated Dry	0.60	0.0	2.0	0.
Cool Irrigated Dry	0.60	0.0	3.0	0.
Cool Grass	0.44	0.0	1.5	0.
Warm Grass	0.44	0.0	1.5	0.1
Savanna	0.53	0.30	1.9	1.0
Bogs	0.60	0.0	2.5	0.1
Mangroves	0.95	0.95	9.0	9.0
Low Shrub	0.85	0.0	4.7	0.1
Mediterranean Types	0.80	0.67	4.3	3.0
Semiarid Woods	0.34	0.0	1.2	0.
Succulent	0.86	0.30	4.8	1.0
Sand Desert	0.0	0.0	0.	0.
Hot Desert	0.15	0.0	0.5	0.
Cool Desert	0.15	0.0	0.5	0.
Tundra	0.55	0.0	2.1	0.
Polar Desert	0.0	0.0	0.	0.
Cool Field/Woods	0.90	0.10	3.	0.
Warm Woods/Field	0.90	0.30	6.	3.
Cool Woods/Field	0.90	0.20	4.	1.
Warm Field/Woods	0.90	0.20	5.	2.
Southern Taiga	0.86	0.0	4.8	0.1
Northern Taiga	0.73	0.0	3.5	0.1
Wooded Tundra	0.70	0.15	3.2	0.5
Heath	0.85	0.0	4.7	0.1
Marsh/Swamp	0.73	0.67	3.5	3.0
Coastal Edges	0.40	0.20	4.	1.
Ice	0.0	0.0	0.	0.
Lakes	0.0	0.0	0.	0.

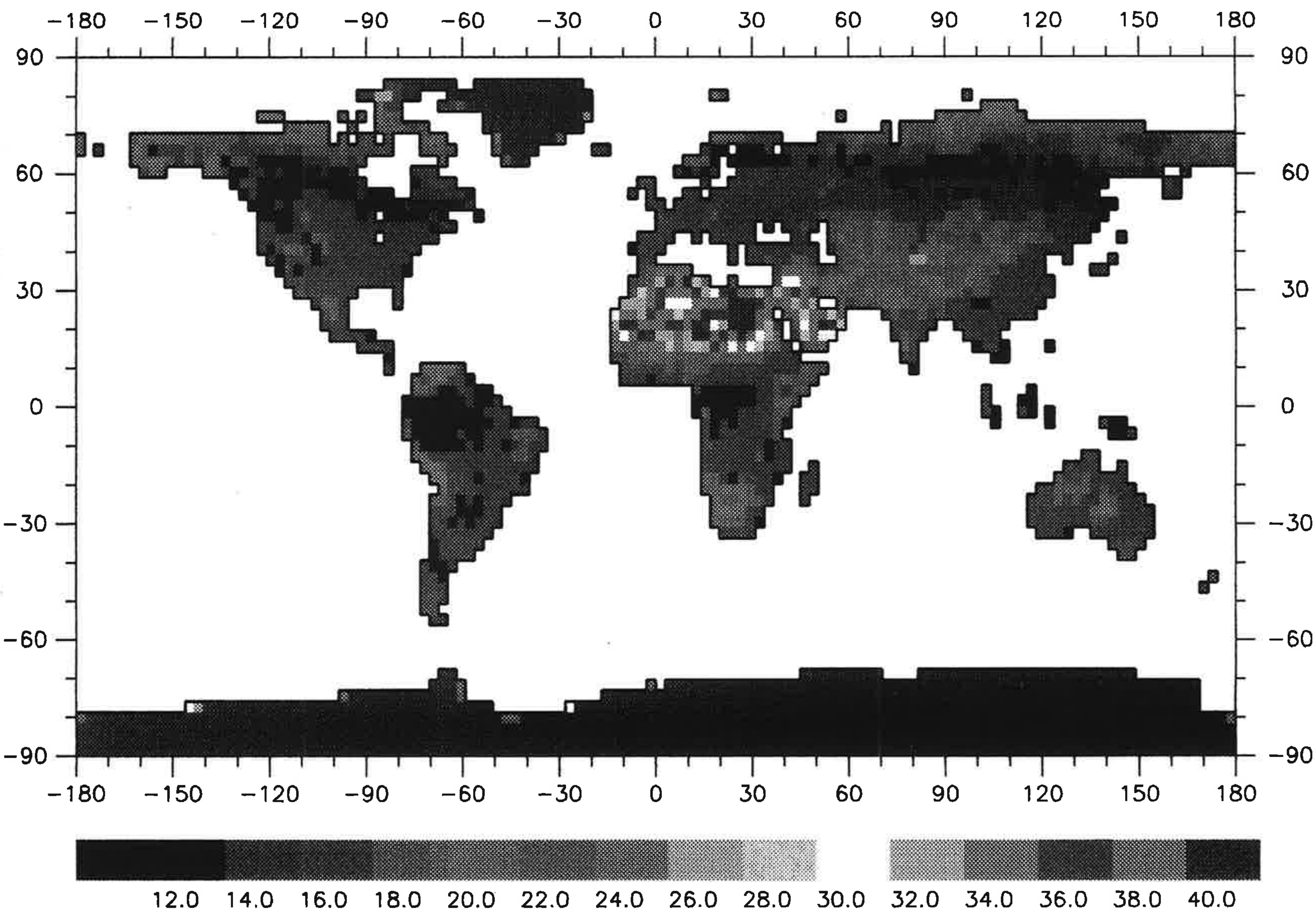

Figure 1: Global distribution of new surface albedo α

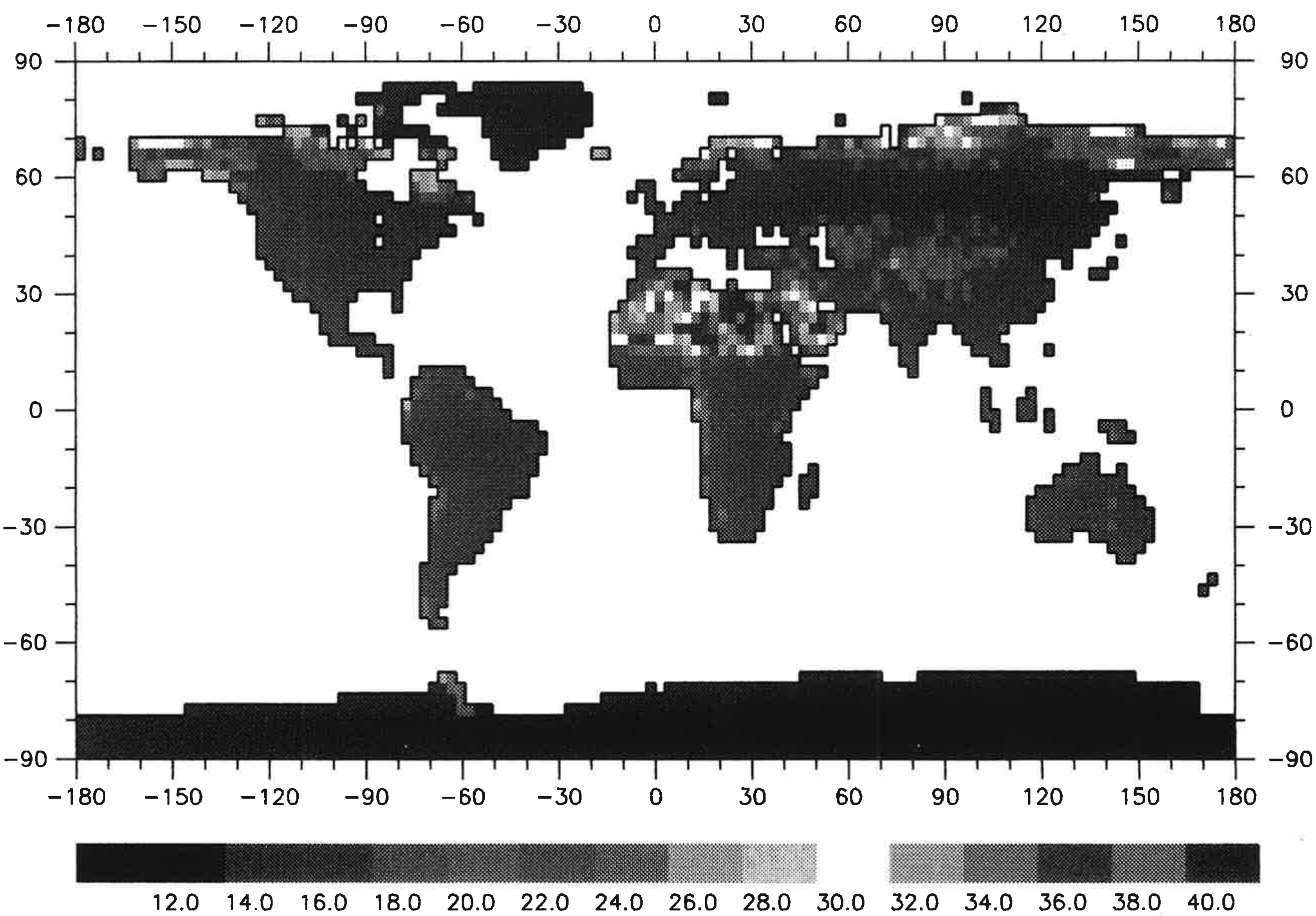

Figure 2: Global distribution of surface albedo used in ECHAM level 3.

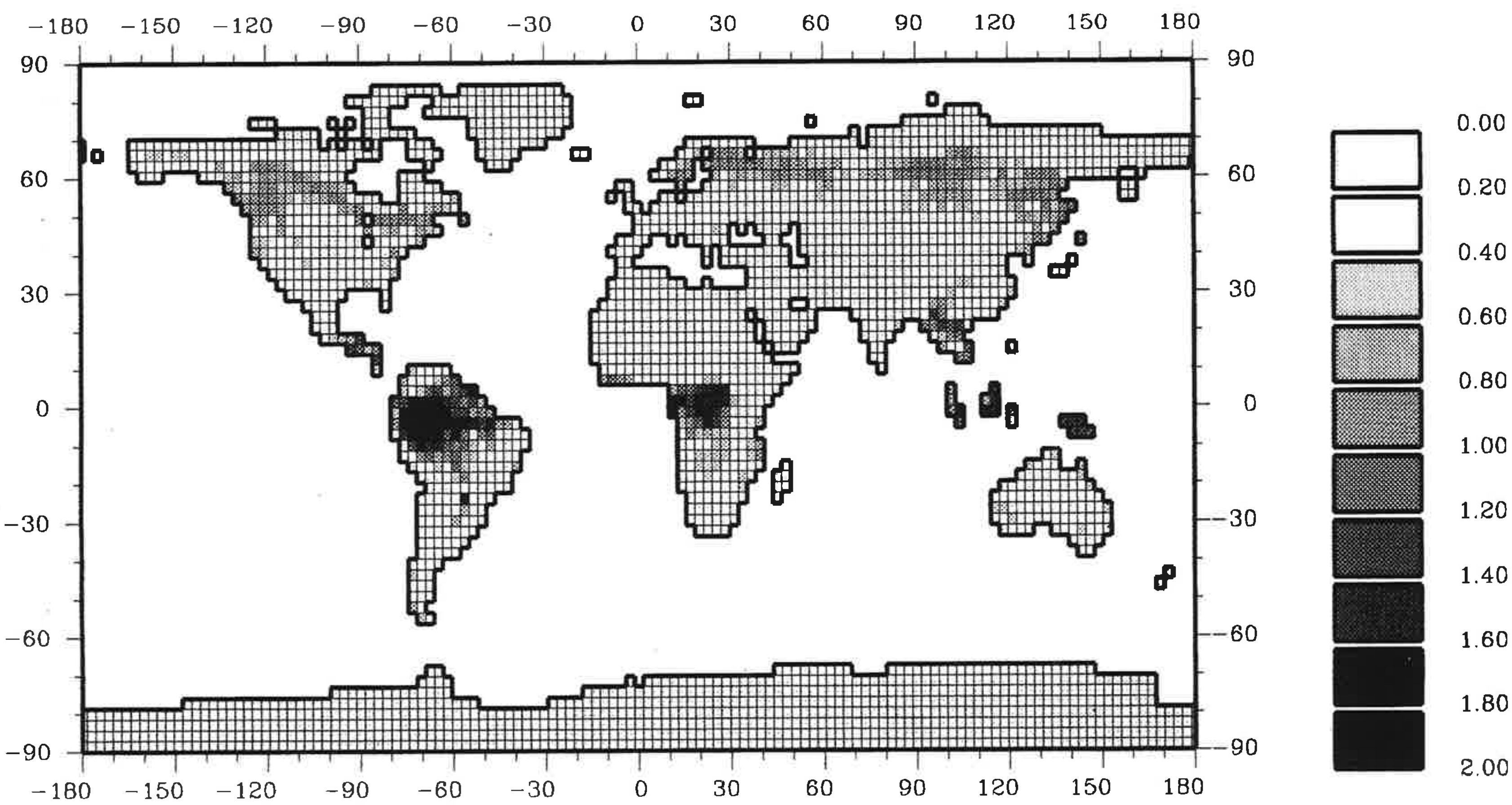

Figure 3: Global distribution of new roughness length z_{0v} of vegetation and land use.

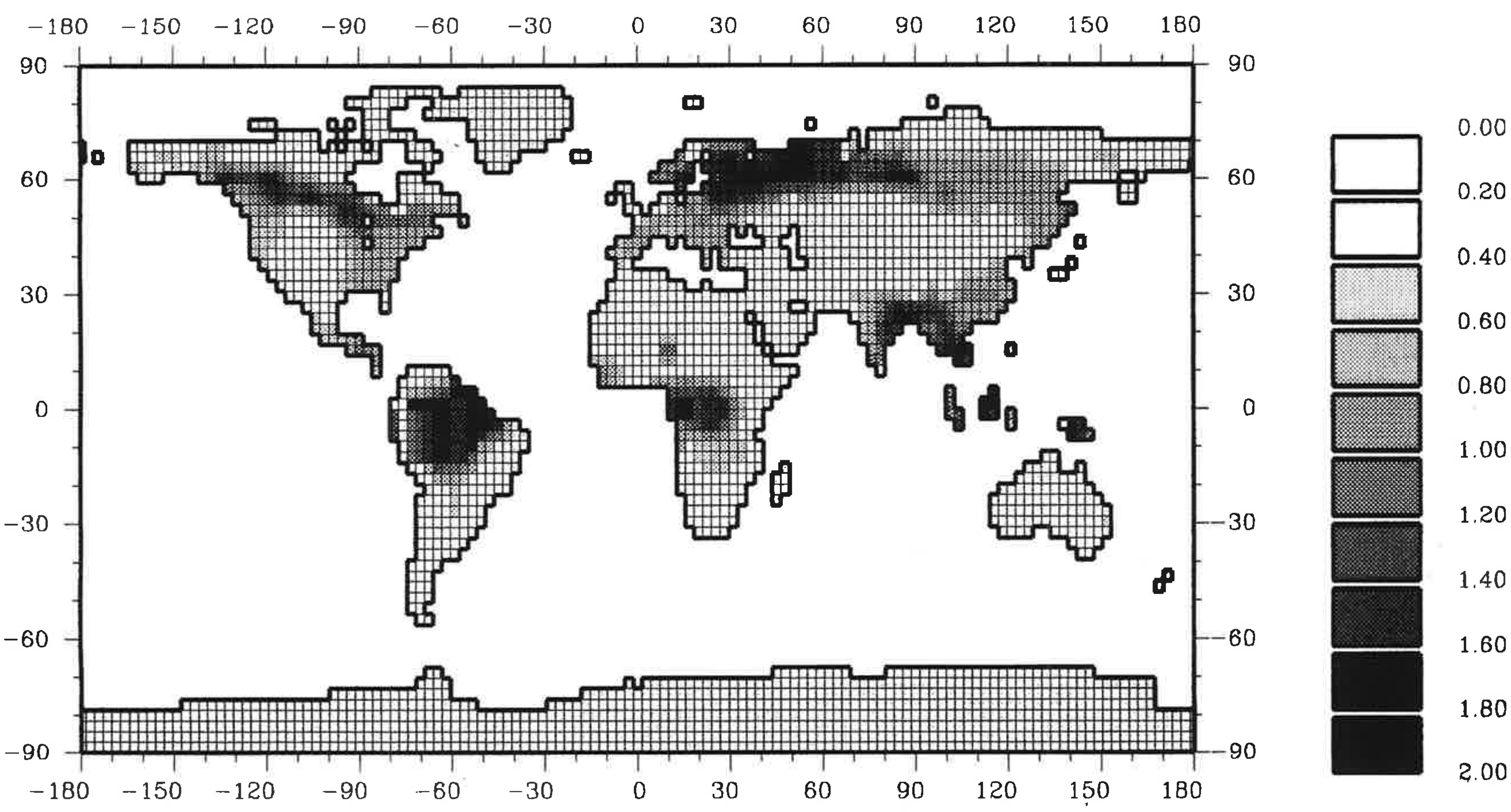

Figure 4: Global distribution of roughness length z_{0v} given by Baumgartner *et al.* (1977).

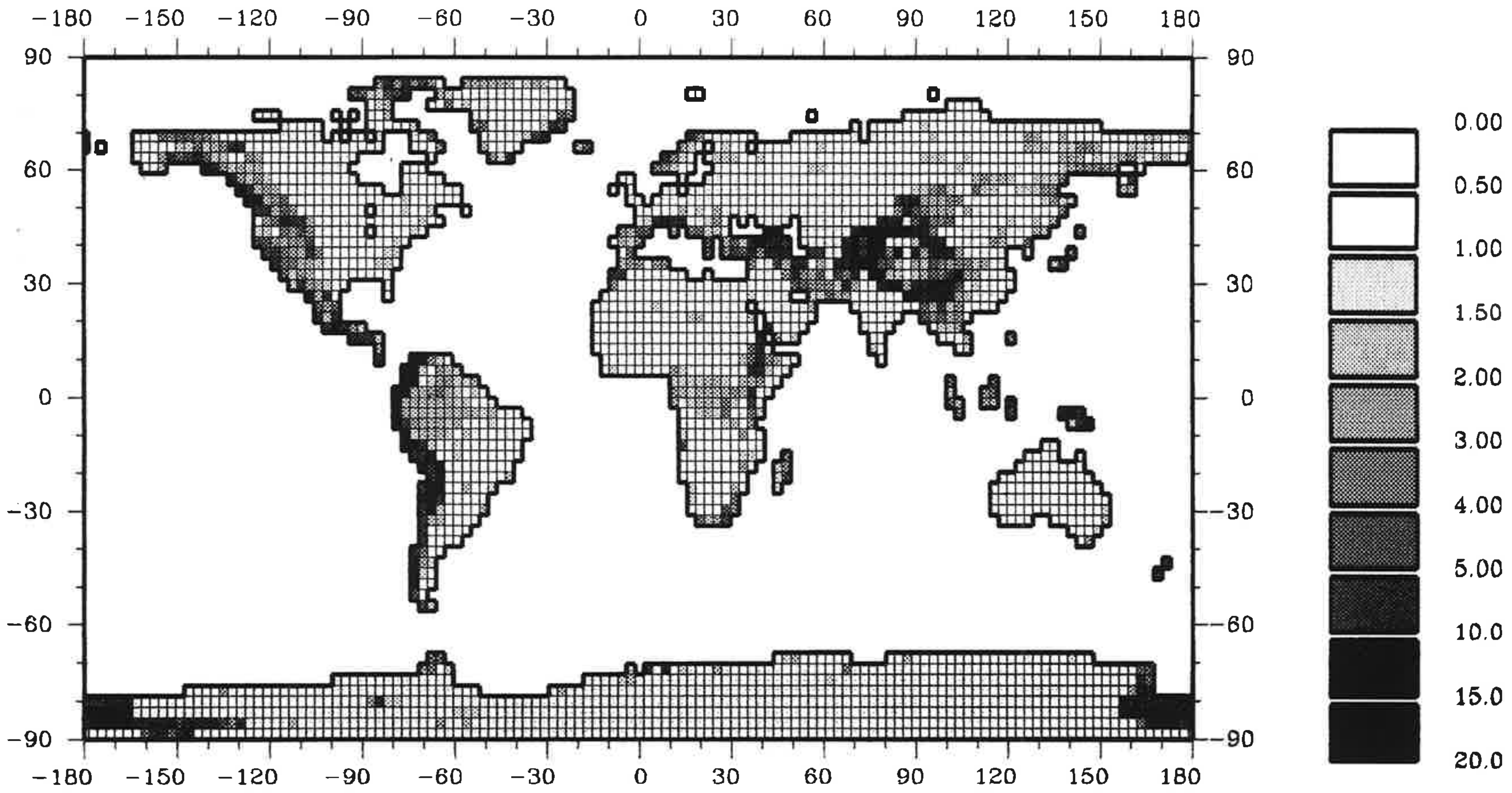

Figure 5: Global distribution of new surface roughness length z_0.

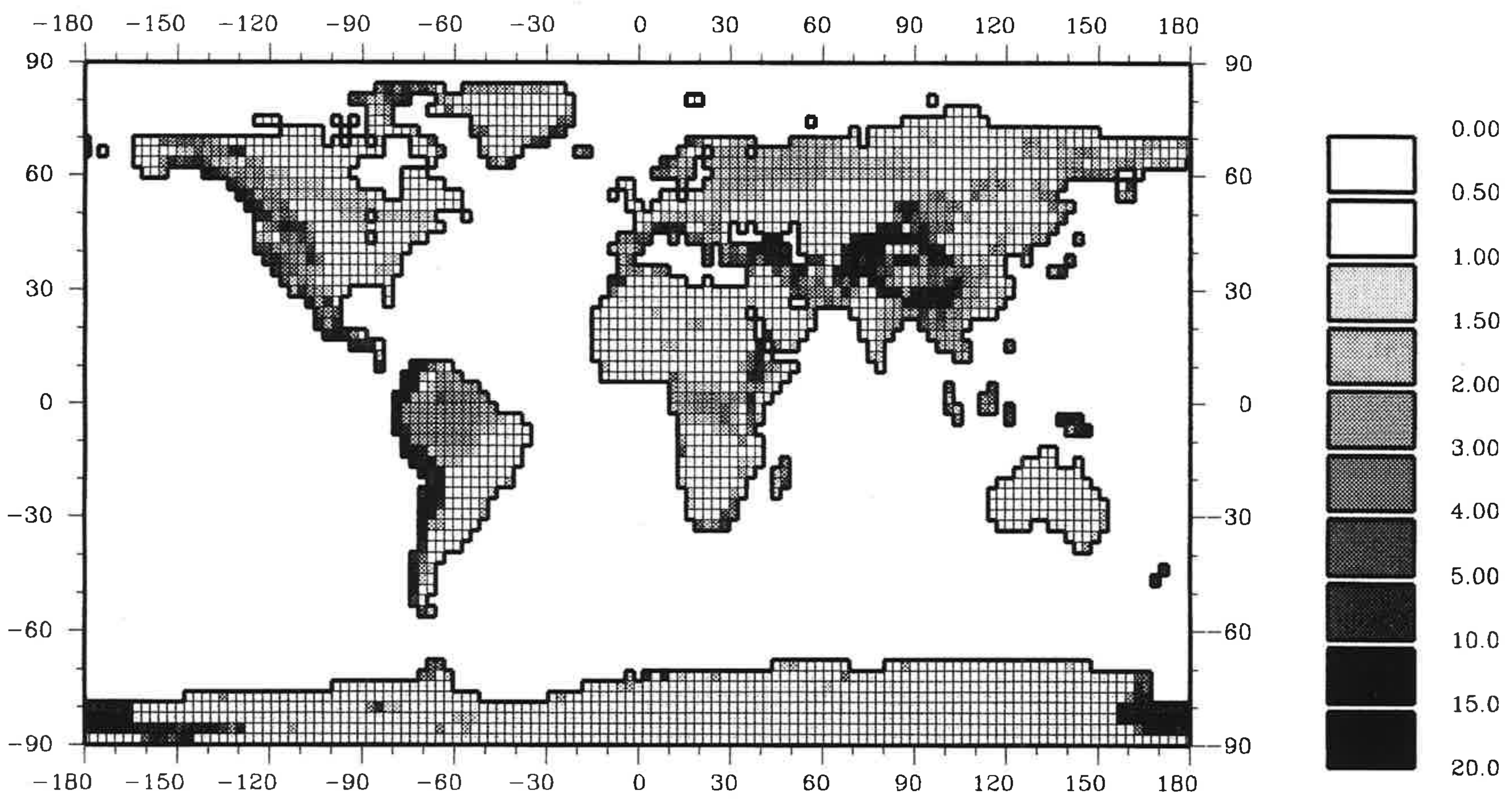

Figure 6: Global distribution of roughness length z_0 used in ECHAM level 3.

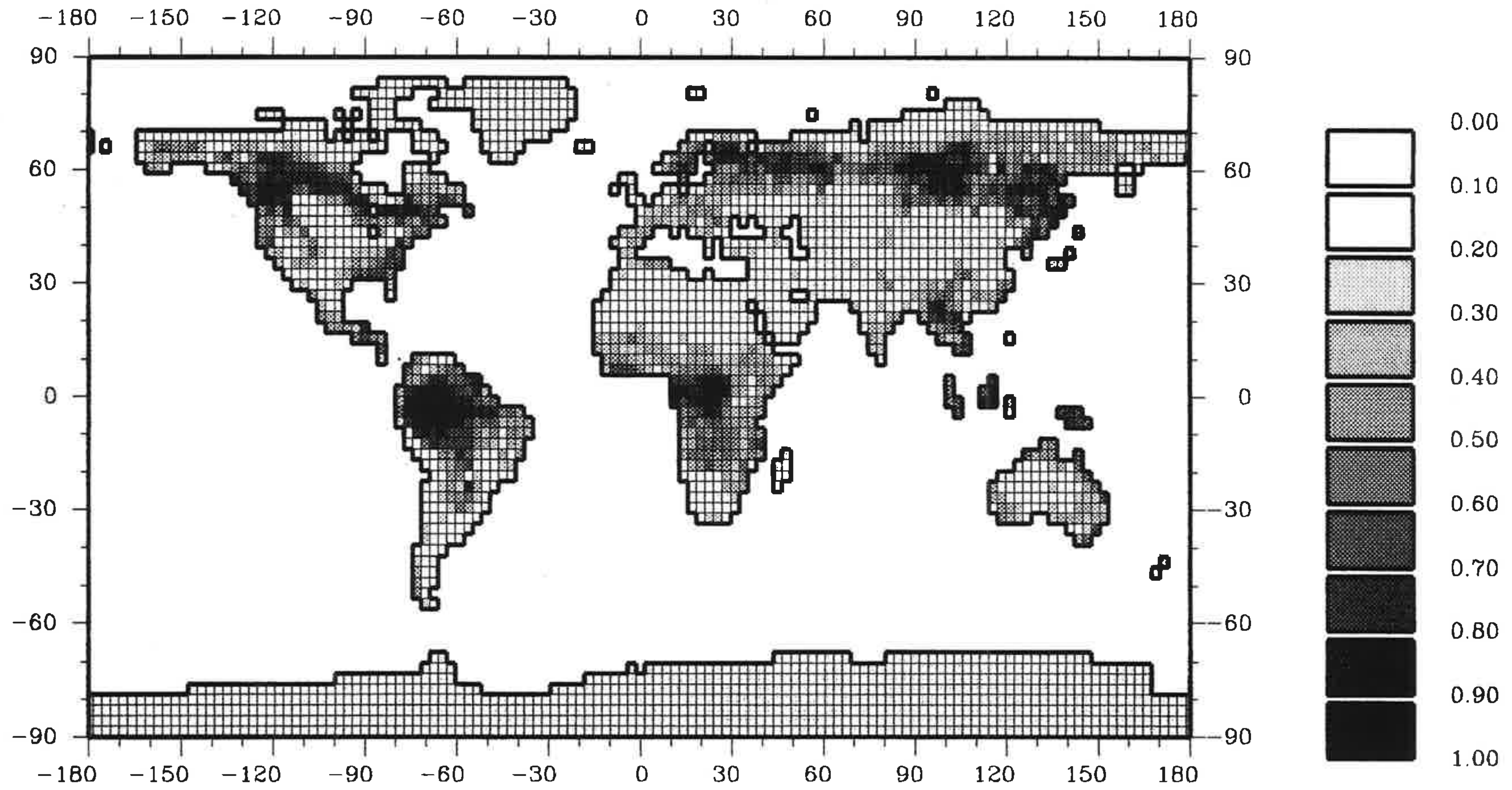

Figure 7: Global distribution of new forest ratio c_F.

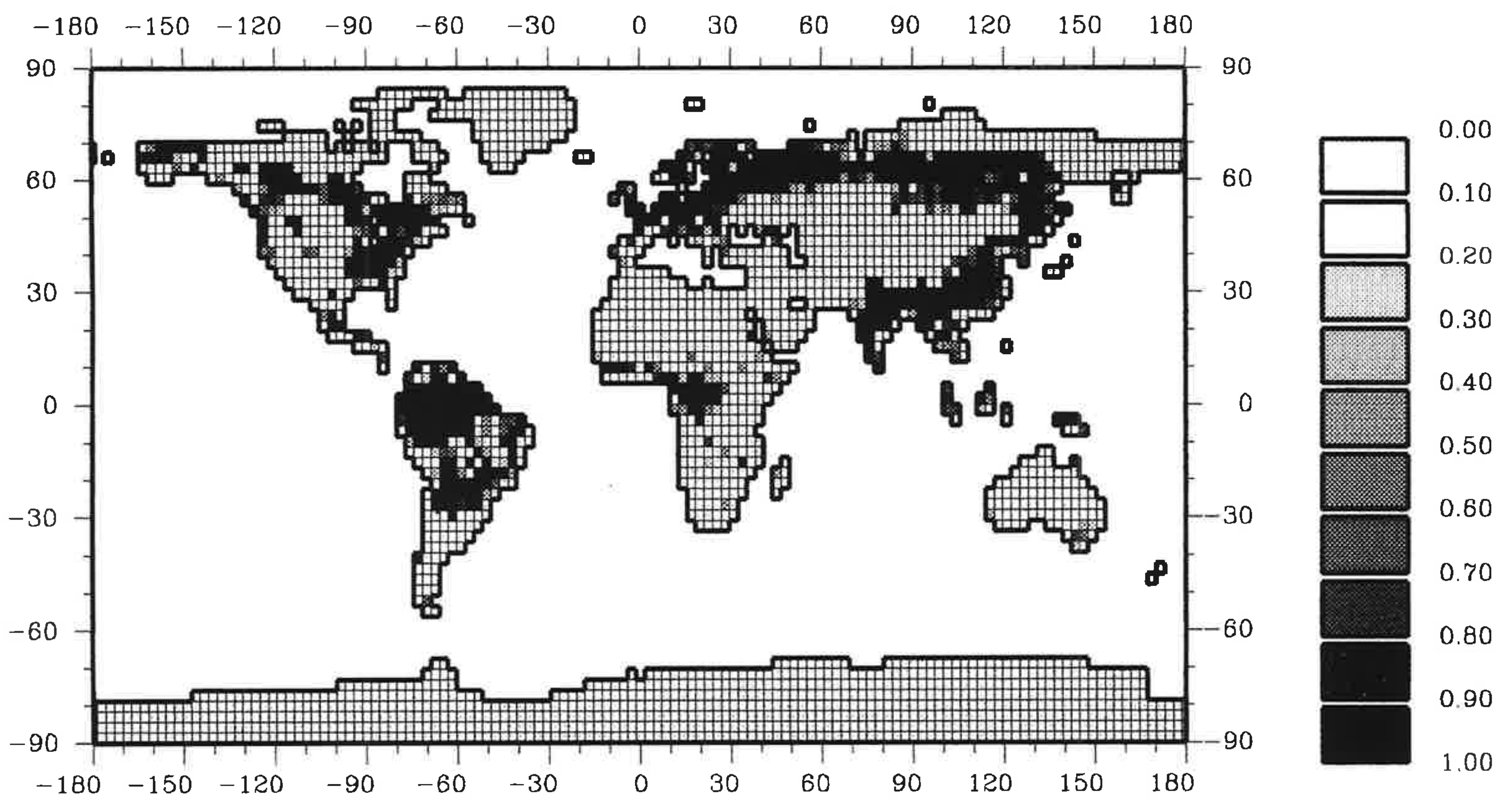

Figure 8: Global distribution of forest ratio derived from Matthews (1984).

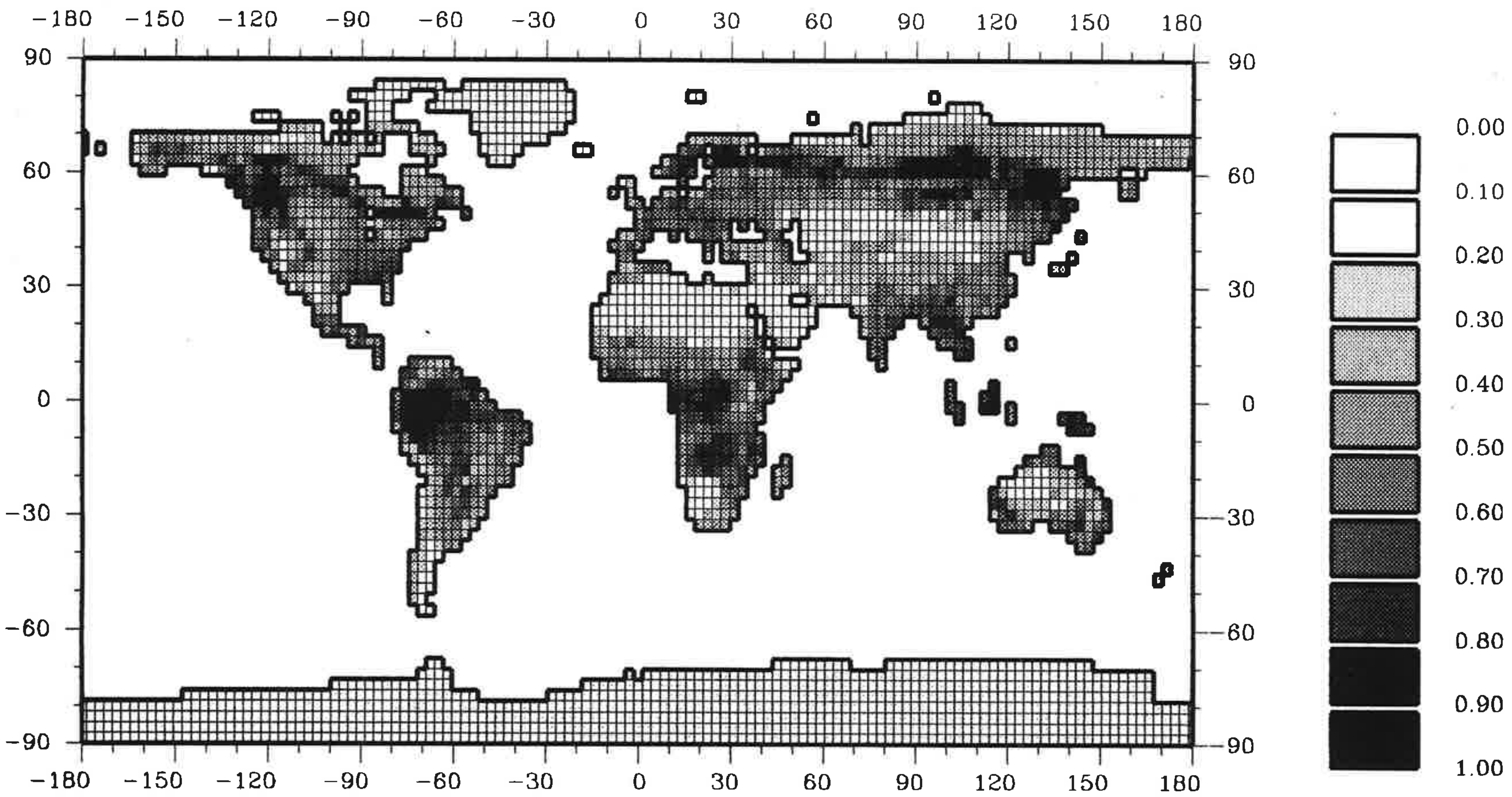

Figure 9: Global distribution of new vegetation ratio c_v.

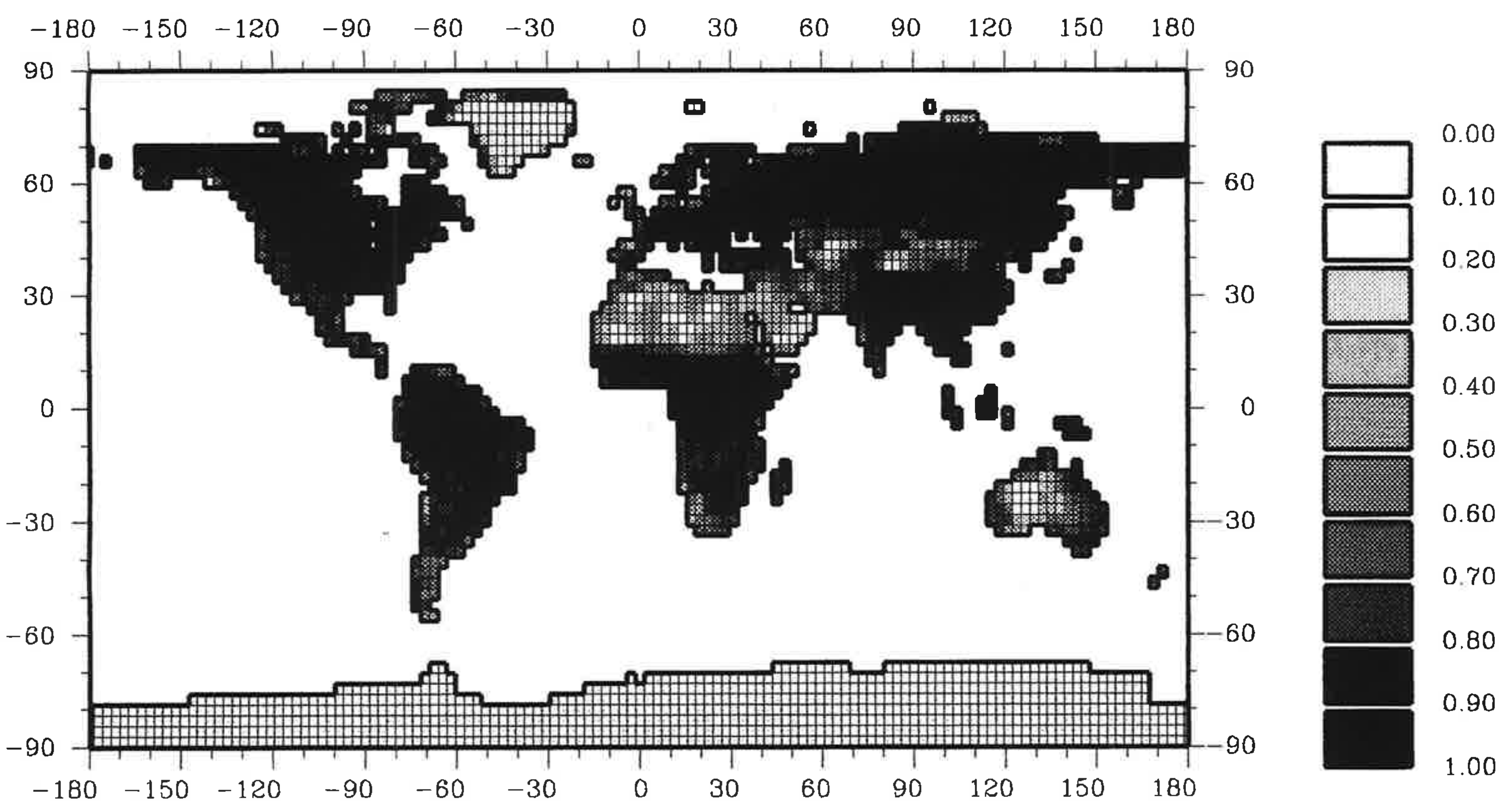

Figure 10: Global distribution of vegetation ratio c_v used in ECHAM level 3.

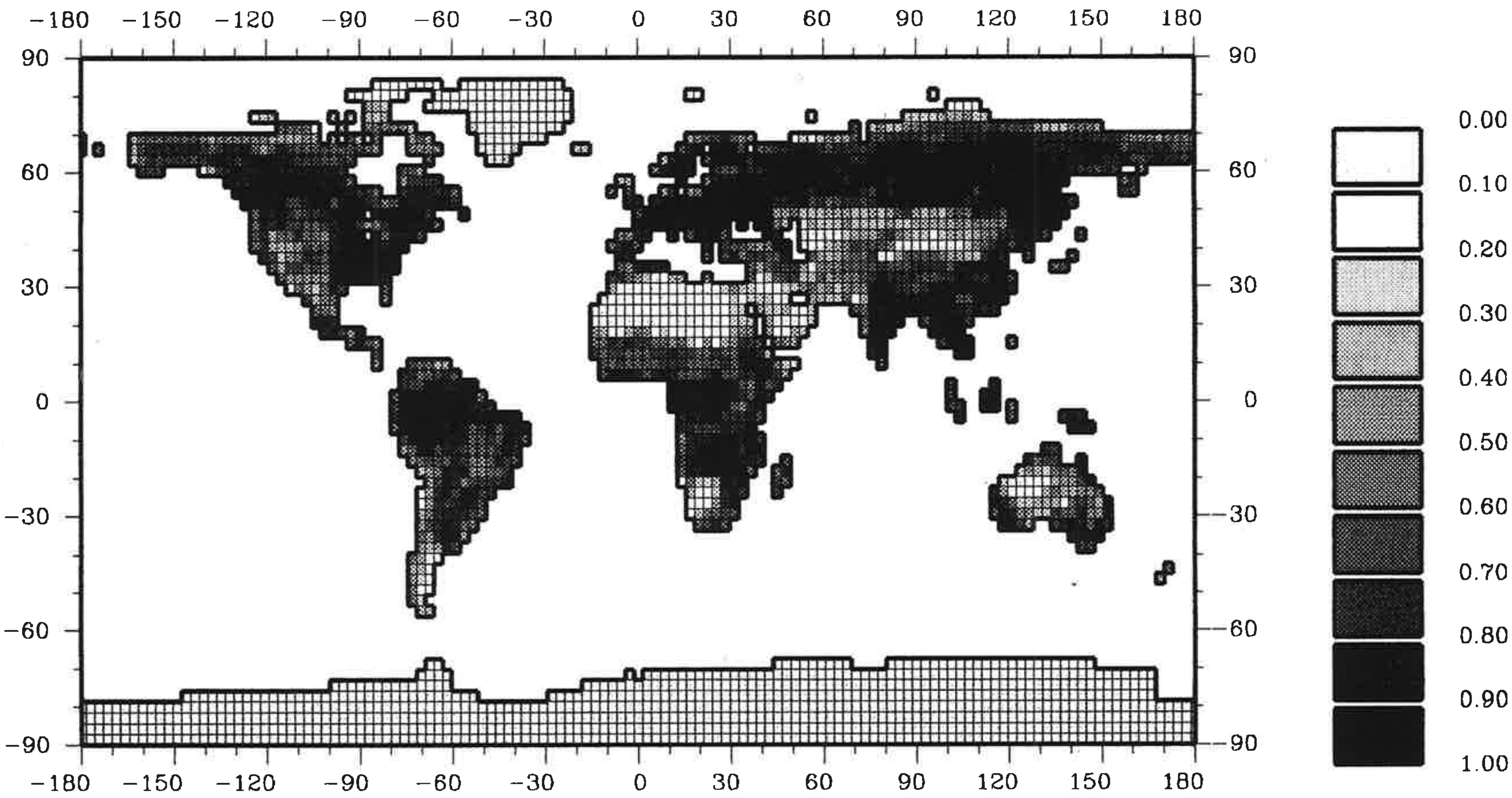

Figure 11: Global distribution of maximum values of c_v.

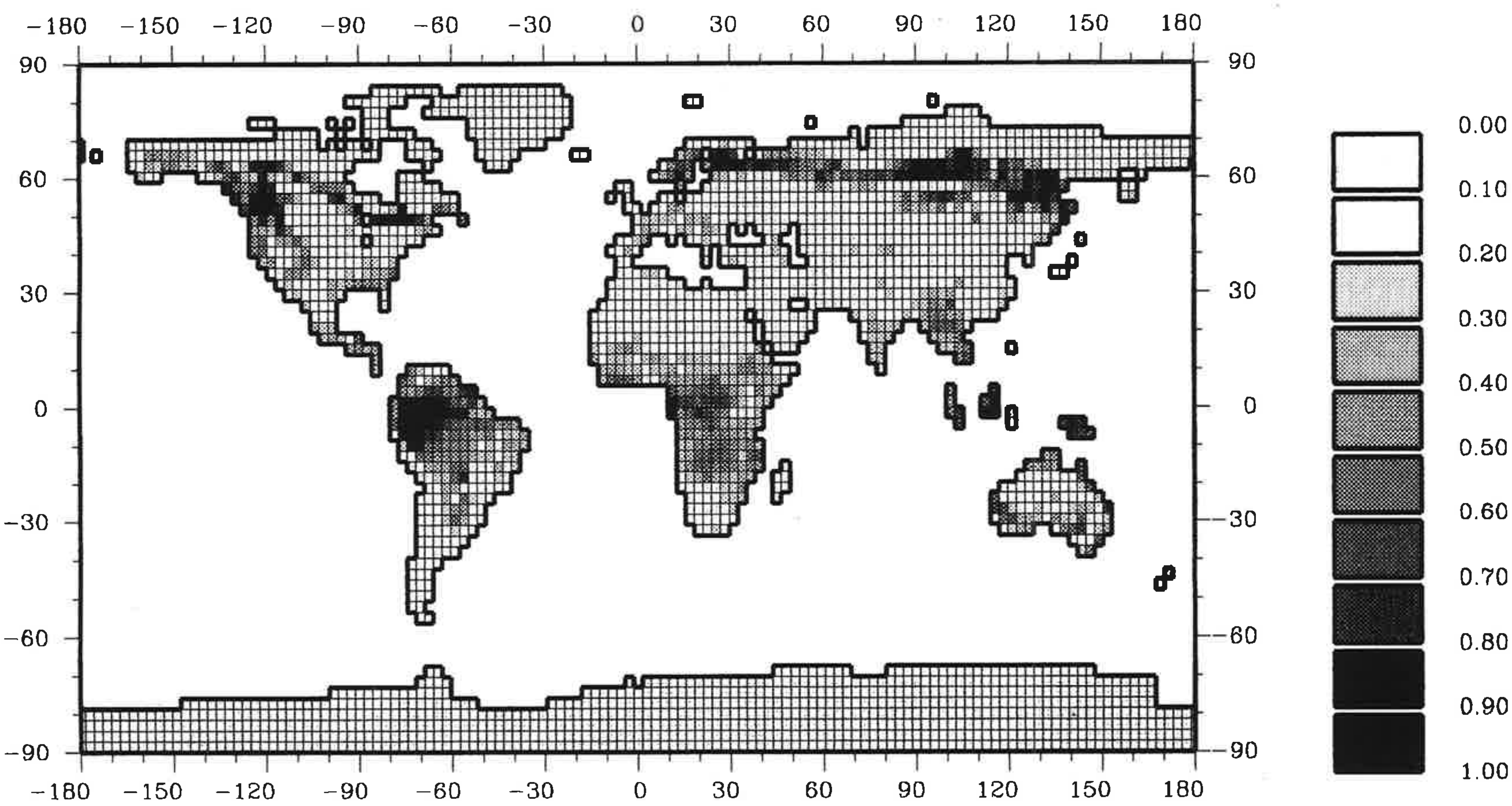

Figure 12: Global distribution of minimum values of c_v.

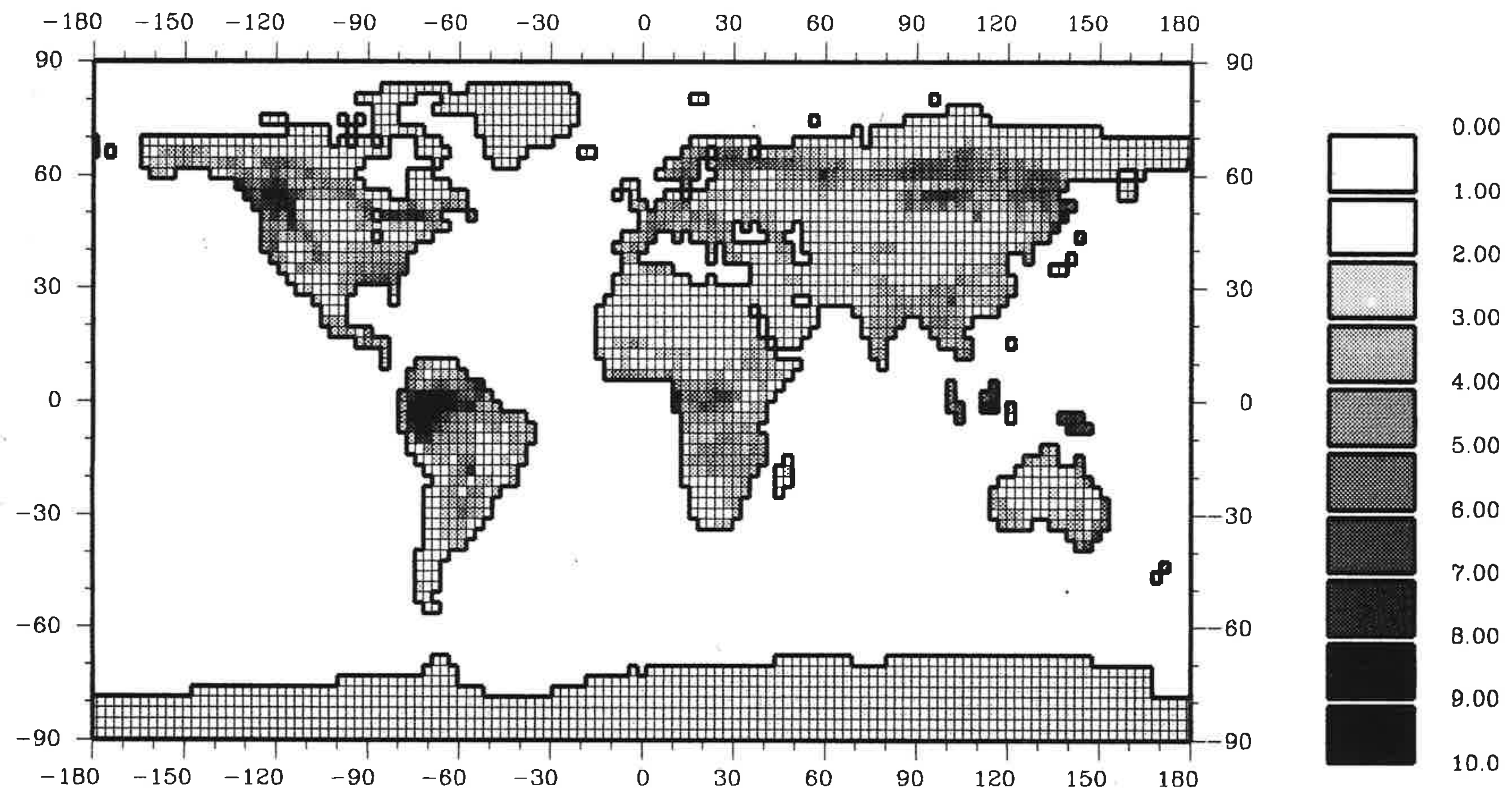

Figure 13: Global distribution of new leaf area index LAI.